Precise Near-Earth Navigation With GPS: A Survey of Techniques

T. P. Yunck, S. C. Wu, and J. Wu

Tracking Systems and Applications Section

The tracking accuracy of low earth orbiters (below ~3000 km altitude) can be brought below 10 cm with a variety of differential techniques that exploit the Global Positioning System (GPS). All of these techniques require a precisely known global network of GPS ground receivers and a receiver aboard the user satellite, and all simultaneously estimate the user and GPS satellite orbits. Three basic approaches are the geometric, dynamic, and non-dynamic strategies. The last combines dynamic GPS solutions with a geometric user solution. Two powerful extensions of the non-dynamic strategy show considerable promise. The first uses an optimized synthesis of dynamics and geometry in the user solution, while the second uses a novel gravity-adjustment method to exploit data from repeat ground tracks. These techniques will offer sub-decimeter accuracy for dynamically unpredictable satellites down to the lowest possible altitudes.

I. Introduction

Tracking requirements for earth sensing satellites, particularly altimetric satellites, are becoming increasingly stringent, reaching the decimeter level for several missions proposed for the 1990s. NASA's Ocean Topography Experiment (Topex) [1]-[3], scheduled for launch at the end of 1991, has a goal of 13 cm altitude accuracy but would benefit from an accuracy level comparable to the 2.5 cm precision of its radar altimeter. A number of similar missions, including the Navy Remote Ocean Sensing System (NROSS) [4], the European Space Agency's Earth Remote Sensing-1 (ERS-1) [5], [6], and a series of altimetry experiments planned for NASA's Earth Observing System (EOS) [7], [8], are also seeking decimeter altitude accuracy.

Topex will carry an experimental tracking system which exploits the U.S. Defense Department's Global Positioning System (GPS) [9], [10]. The basic technique, sometimes called differential GPS, makes use of a high performance GPS receiver on board the orbiter and a small network of precisely located receivers on the ground, distributed roughly evenly around the globe. All receivers continuously observe the visible GPS satellites, making measurements of accumulated RF phase and one-way range at roughly 1.2 and 1.6 GHz (Fig. 1). The one-way range is also called "pseudorange" because it consists of true range plus the time offset between the transmitter and receiver clocks. Orbiter and ground measurements are then combined and processed to recover the orbiter and GPS satellite states in the reference frame defined by the ground network [11]-[19].

For the Topex demonstration, the reference network will include DSN tracking stations in California, Spain, and Australia and at least three complementary sites operated by the Defense Mapping Agency (DMA). A map of the hypothetical

sites used in the error analysis presented here, along with a typical one-orbit Topex ground track, is given in Fig. 2. At Topex launch, ground site relative positions are expected to be known to about 3 cm and their geocentric positions to about 5 cm.

Our purpose here is to evaluate different strategies for applying differential GPS carrier and pseudorange data to determine the user orbit. One requirement of all GPS-based strategies intended to achieve decimeter accuracy is that a joint solution be performed for the user and GPS satellite orbits. If GPS orbits are left unadjusted, user position accuracy is generally limited at the meter level by the a priori GPS orbit error. Because there will be at least 18 GPS orbits to estimate along with the user orbit, considerable data strength is needed for a high accuracy solution.

II. Three Basic Strategies

We begin with three fundamental GPS-based differential tracking strategies: a purely geometric strategy, a fully dynamic strategy, and a combined strategy in which GPS orbit solutions are dynamic and the user solution is geometric. Before presenting the details, a discussion of data combining will be helpful. All of these strategies can use what are called undifferenced, singly differenced, or doubly differenced GPS observables. These correspond, respectively, to the cases in which (1) all clock behavior is modeled over time; (2) GPS clocks are eliminated and only receiver clock behavior is modeled over time; and (3) all clocks are eliminated (or solved for) at each time step. In general, the less differencing applied, the greater the data strength available for orbit solutions. When receiver oscillators are unstable, however, they can seriously degrade the solution by introducing systematic errors. Where possible, it is advantageous in such cases to eliminate oscillator effects through differencing. The analysis presented here assumes the use of doubly differenced data in order to remove oscillators as a possible source of error. Results will invariably improve if oscillators are sufficiently stable to permit less differencing.

A. The Geometric Strategy

This is the differential analog of classical GPS-based point positioning in which a user makes pseudorange measurements to four or more GPS satellites, obtaining a quick geometric solution for position and time offset from GPS time. The conventional (non-differential) user is dependent upon a priori knowledge of GPS satellite positions and time offsets, which for most users are expected to be in error by roughly 5 m. This limits final position error to 10–15 m. In the simple differential approach (Fig. 1), the user and a reference receiver make pseudorange measurements to a common set of at least

four satellites, permitting a geometric solution for the baseline and the time offset between receivers. GPS orbits are left unadjusted, but cancellation of common GPS clock and orbit errors improves user position accuracy to one or two meters.

In the general approach, a network of reference receivers and the user receiver observe the GPS satellites. With sufficient measurements, the user position and all GPS positions can be determined geometrically with respect to the reference ground network. To illustrate, consider a set of four GPS satellites and assume the use of doubly differenced measurements. Including the user, there are 5 satellites or 15 position components to estimate, requiring at least 15 independent doubly differenced measurements. Since each user-to-ground baseline yields three double differences, five baselines and thus five reference receivers are needed, all viewing the same four satellites. If these conditions are met, the user and GPS orbits can be simultaneously estimated, and performance will be limited primarily by measurement precision and observing geometry.

With the current generation of receiving equipment, pseudorange measurements are typically precise to 0.5–1.0 m over one second. This limits instantaneous position accuracy to a meter or worse, depending upon observing geometry. In any geometric strategy, the pseudorange precision limitation can be overcome by introducing GPS carrier phase, continuously counted, and subtracting it from pseudorange, thereby removing receiver and GPS dynamics and permitting pseudorange to be averaged over time. This procedure is known as "smoothing pseudorange against the carrier." More generally, position change obtained from carrier phase measurements can be subtracted from successive position solutions obtained with pseudorange, permitting the averaging of position solutions over arbitrarily long time periods despite frequent switching of GPS satellites. By this means, the general geometric strategy can in principle be made to deliver decimeter accuracy for any low orbiter. In reality, however, an impractically large receiver network is needed to maintain strong determination of all parameters, and therefore the purely geometric approach cannot compete with more efficient alternatives.

B. The Dynamic Strategy

The most familiar of the alternatives is the classical dynamic formulation in which the state parameters at a single epoch are estimated for all satellites using an extended arc of data [11]–[13]. Observations at different times are related to the epoch state parameters by integrating the equations of motion, a process requiring accurate models of the observing system and of the forces acting on the satellites. Errors in the dynamic models naturally introduce errors in the epoch state solution.

In general, the further in time an observation is from the solution time, the greater the expected error from dynamic mismodeling. Consequently, the effect of force model errors tends to increase with increasing arc length.

Compared with the general geometric strategy, this approach vastly reduces the number of estimated parameters, thus increasing data strength and permitting far fewer reference receivers. Moreover, by introducing dynamic constraints, this technique permits solutions that are impossible geometrically, such as the determination of satellite positions from carrier phase (position change) measurements alone. The dynamic technique can therefore be used with carrier phase, pseudorange, or both. These considerable advantages are gained in return for a dependence upon dynamic models, with a consequent vulnerability to modeling errors.

Two recent Topex studies illustrate the importance of accurate models with the dynamic technique. Figure 3 is taken from a covariance study of the altitude error for a single Topex orbit using carrier phase data. Key assumptions include: Topex viewing 4 GPS satellites; integrated doppler data with 0.4 cm noise and 5 min data interval; 6 ground sites known to 5 cm in each component; zenith troposphere calibration accurate to 1 cm; 18-GPS constellation with 4 m a priori ephemeris error. The most critical assumption is the gravity error model, which consisted of the differences between 21 selected coefficients taken from two gravity models, GEM10 and GEM10B [20], [21]. These differences were further reduced by 50 percent to account for expected model improvements before Topex launch. Figure 4 presents a similar analysis (although for a different orbit—note the changed data noise error) which used a gravity model of more than 400 terms differenced between GEML2 [22] and GEM10, this time without the 50 percent reduction. This reflects the approximate accuracy of the best gravity models in the early 1980s. We can see that for a fully dynamic solution strategy, a significant model improvement is needed to reach the Topex 13-cm goal. Efforts over the last several years at the Goddard Space Flight Center and at the University of Texas have led to considerable progress on the gravity model and are expected to result in the achievement of the required accuracy by the time of Topex launch [23].

Although the dynamic strategy looks promising for Topex, were it to be applied at much lower altitudes, such as the 250–350 km typical of shuttle flights, errors would soar. Gravity error would grow substantially and yet would be far surpassed by the greatly increased error in modeling atmospheric drag. In the case of the shuttle, additional complications would arise from the irregular effects of maneuvering and venting. Final orbit error could reach hundreds of meters. For high accuracy at very low altitudes, one is therefore led back to a geometric approach.

C. The Non-Dynamic Strategy

This technique was proposed in 1985 [17] to address specific weaknesses of the two previous techniques. To eliminate significant modeling errors, the user position is once more determined geometrically, with a new and independent solution derived at each time point. To prevent the proliferation of estimated parameters, as occurs with the fully geometric approach, the GPS satellite states are obtained at a single epoch by a conventional dynamic approach. This strategy can be thought of as a classical epoch state dynamic formulation with the user state modeled as process noise with zero correlation time.

Although dynamics appear in this approach, they do so only for the high altitude GPS satellites, for which dynamic modeling errors are negligible. Dynamic treatment of GPS orbits sharply reduces the number of estimated parameters, permitting use of a small reference network. Since the user solution is geometric, the customary dynamic error sources—gravity, drag, solar radiation, maneuvers, and venting, to name a few—are eliminated. In recognition of the geometric user solution, we refer to this technique as *non-dynamic* tracking. Note that in order to obtain a non-dynamic position solution, the pseudorange data type is required. If pseudorange alone is used, however, performance will again be limited at the meter level by the relatively high pseudorange measurement error. The real power of this technique emerges when continuous carrier phase is introduced, allowing the smoothing of position solutions against observed position change. Several hours of smoothing can reduce the contribution of data noise to position error to a few centimeters.

An example from the extensive Topex error studies [17], [18] is shown in Fig. 5. In this case, Topex is assumed to view up to six GPS satellites at once, rather than four. The data noise on the dual frequency, doubly differenced pseudorange is assumed to be 10 cm after a 5 min integration. Other relevant assumptions remain the same. Over a 4-hr data arc, the average altitude error is 7.3 cm, with two peaks of about 12 cm. Several features distinguish this result fundamentally from the dynamic results. Because dynamic model errors are absent, this accuracy can be maintained down to the lowest satellite altitudes (roughly 160 km) without concern for unmodeled forces or possible maneuvering of the vehicle—so long as contact with GPS is not disrupted. Moreover, since there are no user dynamic models to compute, the solution procedure is considerably simpler and faster than with a dynamic approach.

The pseudorange data noise assumed in Fig. 5 corresponds to a single-channel precision of approximately 40 cm in one second. The new "Rogue" receiver now undergoing field tests at JPL improves on this by about a factor of two [15], [24],

while some current commercial receivers have about double this error. Doubling the data noise in Fig. 5 increases the average altitude error to 8.5 cm; halving it reduces the error to 7.0 cm. The receiver to be carried aboard Topex, now being developed by Motorola, is expected to have a pseudorange measurement noise somewhat better than the 40 cm assumed here. It should be noted that for these results to be strictly valid, sources of systematic error such as multipath and instrument delay variations must be contained so that after four hours of averaging their effect is below that of the data noise.

A final point is worth noting. This study assumed a six-receiver reference network and a flight receiver observing up to six satellites. Ground receivers were assumed to track all satellites above 10 degrees. If the flight receiver is restricted to viewing four satellites, as may be the case for Topex, the observing geometry frequently degrades sharply or even breaks down altogether, and errors soar. Enlarging the ground network to 15 sites does not fully restore performance. A more robust strategy to deal with weak geometry is presented in Section IV.

III. Carrier Range

There is a data type called "carrier range" which is sometimes recoverable from differential GPS observations. Carrier range is obtained by determining the exact number of full cycles in the carrier phase observable differenced between two receivers. It is, in effect, a differenced pseudorange having the sub-centimeter precision of carrier phase measurements. The process of determining the integer cycle count is called cycle ambiguity resolution or "bias fixing," and a variety of techniques have been devised to carry it out [15], [25], [26]. Bias fixing is a demanding task that currently can be reliably achieved only between fixed ground sites no more than a few hundred kilometers apart. Several groups are now trying to achieve bias fixing over continental distances.

Carrier range performance can often be approached with the combined carrier phase and pseudorange data types. Carrier phase has the precision of carrier range without the position information; pseudorange has the position information without the precision. Over long data arcs, pseudorange error can be averaged down to bring the effective data noise near that of carrier range. Other errors tend to mask the remaining difference.

Consider, for example, the non-dynamic analysis with combined data types shown in Fig. 5. The same case using carrier range, shown in Fig. 6, yields an average improvement of 1.3 cm. (To optimize performance in Fig. 6, three ground sites were adjusted. Without this refinement, there is no net improvement.) When the assumed pseudorange error is halved to

correspond to that of the best GPS receivers, the carrier range advantage is reduced to 1.0 cm. Thus, if bias fixing proves to be unattainable over long distances, the combined data type may offer a practical alternative. Again we must stress that in precise applications of pseudorange, multipath must be carefully controlled.

IV. Two Advanced Strategies

The non-dynamic strategy has an important limitation: Performance is strongly dependent upon the momentary observing geometry, as evidenced by the error fluctuations in Fig. 5. The momentary observing geometry depends in turn upon the number and arrangement of ground receivers, the receiver viewing capacities, and the GPS satellite constellation. Loss of a key ground site, GPS satellite, or user channel can cause the solution to degrade sharply or even fail altogether. One way to address this is by reintroducing user dynamics, appropriately weighted according to model quality, while preserving the essential geometric technique. With this approach, which is developed in detail below, user dynamics smooth the solution through geometric trouble spots while adding information and strength throughout.

A. The Reduced Dynamic Strategy

To put this idea into practice, we return to the dynamic formulation and introduce a non-dynamic component to the solution by incorporating added process noise in the user force models. The GPS state solution remains fully dynamic, while the user solution is, in general, partly dynamic and partly non-dynamic. Widely different solution characteristics, ranging from fully dynamic to non-dynamic, can be achieved simply by varying the parameters defining the process noise. The solution can be optimized for a particular combination of geometric strength and dynamic model accuracy by careful tuning of those parameters.

We present this "reduced-dynamic" technique mathematically in a Kalman sequential filter formulation. This involves two steps: a *time update*, which makes use of a state transition model to propagate the satellite state estimate and covariance from one time batch to the next, and a *measurement update*, which incorporates a new batch of measurements. These two steps alternate until all data batches are incorporated.

In the *time update*, let $\hat{x}_j$ be the user satellite state estimate at time t_j using data up to the time t_j, and $\tilde{x}_{j+1}$ the predicted state estimate at time t_{j+1} using data only up to t_j; let $\Phi_x(j+1,j)$ denote the state transition from t_j to t_{j+1}. We now introduce process noise parameters p representing a fictitious 3-D force on the user satellite. This gives us the following dynamic (state

32

transition) model for the augmented state $\mathbf{X} = [\mathbf{x}, \mathbf{p}]^T$ and its associated covariance P [27]:

$$\widetilde{\mathbf{X}}_{j+1} = \Phi_j \widehat{\mathbf{X}}_j + B\mathbf{w}_j \qquad (1)$$

and

$$\widetilde{P}_{j+1} = \Phi_j \widehat{P}_j \Phi_j^T + BQ_jB^T \qquad (2)$$

where

$$\Phi_j = \begin{bmatrix} \Phi_x(j+1,j) & \Phi_{xp}(j+1,j) \\ 0 & M_j \end{bmatrix} \qquad (3)$$

and

$$B = \begin{bmatrix} 0 \\ I_p \end{bmatrix} \qquad (4)$$

In Eq. (3), $\Phi_{xp}(j + 1, j)$ is the transition matrix relating $\widetilde{\mathbf{x}}_{j+1}$ to the process noise parameters $\mathbf{p}_j$, and M_j is a 3×3 diagonal matrix with its ith element

$$m_i = \exp\left[-(t_{j+1} - t_j)/\tau_i\right] \qquad (5)$$

In the above equations, $\mathbf{w}_j$ is a white noise process of covariance Q_j which is also diagonal with its ith element $q_i = (1 - m_i^2)\sigma_i^2$, and I_p is a unit matrix. Both the steady-state uncertainty σ_i and the correlation time constant τ_i can be selected to be the same for all i in this application; thus we will drop the subscript i. The relative weighting of the dynamics is varied by selecting different values for the a priori uncertainty σ_0, the steady-state uncertainty σ, and the correlation time τ for these process-noise parameters. Increasing τ and decreasing σ_0 and σ increases the weight on the dynamic information. When $\tau \to \infty$, $\sigma \to 0$, and $\sigma_0 \to 0$, the technique reduces to conventional dynamic tracking; when $\tau \to 0$, $\sigma \to \infty$, and $\sigma_0 \to \infty$, it becomes non-dynamic tracking. It follows that an optimally tuned reduced-dynamic solution must always be as good as or better than both the fully dynamic and the non-dynamic solutions.

The model for a *measurement update* in the reduced-dynamic technique is the same as that for conventional dynamic or non-dynamic tracking, with the exception that $\mathbf{X}$ and P are now associated with the augmented state. Thus,

$$\widehat{\mathbf{X}}_j = \widetilde{\mathbf{X}}_j + G_j(\mathbf{z}_j - A_j \widetilde{\mathbf{X}}_j) \qquad (6)$$

and

$$\widehat{P}_j = \widetilde{P}_j - G_j A_j \widetilde{P}_j \qquad (7)$$

where $\mathbf{z}_j$ is the measurement vector at time t_j; A_j is the matrix of the corresponding measurement partials with $\mathbf{X}_j$; and G_j is the Kalman gain given by

$$G_j = \widetilde{P}_j A_j^T (A_j \widetilde{P}_j A_j^T + R_j)^{-1} \qquad (8)$$

with R_j being the error covariance of $\mathbf{z}_j$. These models are formulated in terms of current state for clarity. A pseudoepoch state U-D factorized formulation [27] has been implemented in the GPS error analysis software known as OASIS (Orbit Analysis and Simulation Software) developed at JPL [28].

1. Performance analysis. Further insight into the reduced-dynamic technique can be gained by comparing its performance in all its key forms, including fully dynamic, optimized reduced dynamic, and non-dynamic. For this analysis we assume a constellation of 18 GPS satellites in six orbit planes, with pseudorange and accumulated carrier phase measurements acquired by Topex and six ground receivers every 5 minutes. Data noise, after dual frequency combination, is set at 5 cm and 0.5 cm, respectively, for the two data types. Carrier phase biases, which must be estimated in the solution process, are given large a priori uncertainty. A 2-hour data arc covering a full Topex orbit is used in all cases. The Topex ground track and positions of the six ground sites are again those of Fig. 2. Other error sources considered are given in Table 1.

To eliminate systematic oscillator error, the clocks at all GPS satellites and at all but one ground site are modeled as white process noise and estimated at each time step. This is a general form of the double differencing technique discussed in Section II. Earth gravity error is represented by a lumped model of a 20×20 field derived by taking 50 percent of the difference between two earth models, GEM10 and GEML2. Comparisons of this representation with the estimated accuracies of the best current gravity models suggest that this error model somewhat overstates the true error by perhaps 20 or 30 percent. The 1-cm zenith troposphere error given in Table 1 assumes the use of a water vapor radiometer at each ground site. Both Topex and the ground receivers are assumed to observe all GPS satellites within their fields of view (typically 6 or 7) unless otherwise stated. The relative performance of the different filter methods is assessed by comparing the estimated Topex altitude errors over the entire 2-hour span. For this, the state covariances of Topex are first smoothed backward and are then mapped to all time points when data

are taken. Comparison is made between the root-mean-square (RMS) errors calculated over these time points.

In preliminary studies not shown here, the properties of the two limiting cases of the reduced-dynamic technique were confirmed. With τ set to 0 and both σ_0 and σ set to a large number, the error estimate, as expected, approaches the solution derived from a separate non-dynamic formulation. When τ is large and both σ_0 and σ are set to 0, the purely dynamic result is produced. Now let's examine a series of intermediate values for τ, σ_0, and σ. The results, in general, will vary with the batch-to-batch uncertainty $\sigma_{bb} \equiv (1 - m^2)^{1/2}\sigma$ rather than with the steady-state uncertainty σ and τ individually. Therefore, in the following analysis a constant $\tau = 15$ minutes is used; only $\sigma_0 = \sigma$ is varied to yield a nearly optimal solution.

Figure 7 shows the Topex altitude error as a function of the percentage of the GEM10-GEML2 error for various values of σ. This includes the results for dynamic tracking ($\sigma = 0$, $\tau \to \infty$) and non-dynamic tracking ($\sigma \to \infty$, $\tau = 0$). It is clear that for any finite dynamic model error (in this case dominated by the gravity), a range of σ exists with which Topex altitude error is lower than with either the dynamic or the non-dynamic solution. In other words, the reduced-dynamic technique is superior provided that the dynamic model is properly weighted.

In Fig. 8, the reduced-dynamic solution is compared with the dynamic and non-dynamic solutions for three different observing capacities for the GPS receiver on board Topex: simultaneously observing 4 GPSs, 5 GPSs, and all GPSs (typically 6, and seldom more than 7) above the Topex horizon, which is defined to be 90 degrees from zenith. In the cases with restricted receiver capacity, satellites are selected to minimize switches over the observing period, thereby maximizing continuity in carrier phase measurements while maintaining good observing geometry (low PDOP). The gravity error is fixed at 50 percent of the difference between GEM10 and GEML2, which is roughly the level of our current uncertainty. A near-optimum weight ($\sigma = 0.5$ μm/sec^2) is used for the reduced-dynamic solution in all three cases.

With a Topex receiver observing all visible satellites, the geometry is always good and non-dynamic tracking is powerful; incorporating the extra dynamic information using the reduced-dynamic technique improves the accuracy by only 1 cm. An improved gravity error, perhaps achieved through gravity tuning with Topex data, would of course improve the reduced-dynamic technique. At the other extreme, with Topex observing only 4 satellites, the geometry is often poor, and non-dynamic tracking performance is much worse than that of dynamic tracking. The reduced-dynamic combination

therefore offers little improvement over purely dynamic tracking. If the gravity error is doubled, however, as in the case of a lower orbit, dynamic tracking error nearly doubles, to 24 cm, while reduced-dynamic performance degrades only moderately, to 16 cm. The third case, Topex observing 5 satellites, falls between these extremes. Dynamic tracking and non-dynamic tracking give 12 and 16 cm, respectively. The reduced-dynamic combination improves this to 9 cm, illustrating the clear advantage of reduced-dynamic tracking when dynamic and non-dynamic performance levels are comparable.

Dynamic tracking naturally yields higher error over regions where gravity is poorly known, e.g., over ocean basins. Non-dynamic tracking, on the other hand, is vulnerable to poor observing geometry. In the reduced-dynamic combination, the two techniques complement one another; the weakness of each is covered by the other's strength, and the solution is better balanced. This is illustrated in Fig. 9, which compares Topex altitude determination accuracy over the whole orbit (2 hours) using the three techniques. A Topex receiver observing up to 5 satellites and the 50 percent GEM10-GEML2 gravity error are assumed. Both dynamic and non-dynamic solutions show peak errors of 25 cm or higher at some points. The reduced-dynamic solution using a near-optimum weight ($\sigma = 0.5$ μm/sec^2) smooths these peaks and remains below 13 cm for the whole 2-hour period. Reduction of the error peaks is the result of a near-optimum trade of state transition information between the dynamic and non-dynamic approaches.

At times when the transition information of one approach is poor, the least-squares estimation filter shifts weight to the other, minimizing the overall error. To illustrate this, Fig. 10 breaks down the Topex altitude error at three times when either the dynamic or the non-dynamic technique performs poorly. The near-optimum trade of state transition information in the reduced-dynamic solution has yielded a more uniform contribution from all error components.

The robustness of the reduced-dynamic technique was further demonstrated in an independent study by Williams [8] that investigated an example of temporary data outage during which the non-dynamic technique failed to produce a useful solution. In the same situation, the reduced-dynamic technique automatically shifts full weight to the dynamics, with the result that there is no noticeable loss of accuracy during the outage provided it does not last too long.

Up to this point, a data arc of only 2 hours has been used. In general, with any solution technique, the effects of data noise, station location, and troposphere are naturally reduced as the data arc length increases. With conventional dynamic tracking, the effects of dynamic error typically *increase with* arc length and eventually begin to dominate. As a result, it is

usually necessary to choose a compromise arc length that balances data errors and dynamic errors. With the reduced-dynamic technique, however, this is not the case. As the arc length increases, the data strength increases; as a natural consequence of the estimation process, the reduced-dynamic technique then shifts greater weight to geometry in such a way as to maintain the balance between data errors and dynamic errors. In effect, dynamics are continuously deweighted as the arc length increases in order to take advantage of the growing data strength. No change in σ is needed for this, since the optimum σ applies to a specific dynamic model error independent of data span. As a result, with optimal weighting the overall performance will not degrade, and will generally improve, with increased data span.

To demonstrate this, Fig. 11 compares the Topex altitude error using 2-hr and 4-hr data spans. The longer data span reduces the error to less than 10 cm over the entire 2-hr period. The RMS altitude error is 7 cm, as compared to 8.9 cm for the 2-hr tracking. An examination of the error breakdown shows a reduction in gravity error as well as in other errors. Although data spans longer than 4 hours have not been studied, it is expected that the error will reduce monotonically with data span. Owing to reduced weight on the dynamic model with longer data span, a reduced-dynamic solution will gradually become a non-dynamic solution as the span is increased. Note that this is true only under the assumption that a fixed, pre-determined dynamic model is used, independent of the data arc length. If the gravity model is steadily improved through tuning or other efforts, the optimum weight for a given data span will shift toward a more strongly dynamic solution.

2. **Weighting the dynamic model.** To benefit fully from the reduced-dynamic technique, the weight on the dynamic model, specified by σ with any adopted τ, must be near its optimum value. However, the sensitivity to a departure from optimum weighting appears to be low. This is illustrated in Fig. 12, which plots the orbit error as a function of the level of gravity error for five different values of weighting, assuming a 5-satellite Topex viewing capacity (compare Fig. 7). The curves for $\sigma = 0.125$ μm/sec^2 and $\sigma = 2$ μm/sec^2 intersect at a gravity error of about 42 percent of GEM10–GEML2. The optimum weight at that point is $\sigma = 0.5$ μm/sec^2. These three curves form a shallow triangle which lies nearly horizontal. Even with σ a factor of 4 from the optimum, Topex altitude error increases by only 0.6 cm. In other words, performance is insensitive to σ near the optimum.

For a particular application, the proper weight can be estimated in advance through a covariance analysis using a realistic dynamic error model. Misjudgment of dynamic error will, of course, yield a suboptimal weight. Care can be taken, however, to minimize the resulting error. The following is a simple strat-egy: Use a nominal dynamic error model to predict the performance of both dynamic and non-dynamic techniques. If either technique is clearly superior to the other—say, by a factor of 3 or more—the slight improvement that would result from combining the two approaches with the reduced-dynamic technique may not justify the extra effort (although the enormous advantage of having dynamics to fill in when geometry fails, say, as a result of a hardware failure, argues against eliminating dynamics altogether). If neither technique is clearly superior, a weight departing from the predicted optimum in a direction favoring the non-dynamic technique (i.e., with a larger σ) should be chosen. The "biased" weighting reduces the more damaging effect when gravity error actually is larger than expected.

This is illustrated in Fig. 13, which shows Topex altitude error, again for three reduced dynamic weights, over a wider range of gravity error. The dotted line shows the possible performance with optimal weight. Suppose the nominal gravity error is 42 percent of the difference between GEM10 and GEML2. The weight $\sigma = 0.5$ μm/sec^2 is nearly optimal at this value. If the actual gravity error is, for example, a factor of 2.4 larger (100 percent GEM10–GEML2), this weight would degrade the altitude determination from 9.7 cm at its true optimum ($\sigma = 2$ μm/sec^2) to 12.3 cm. A weight favoring the dynamic approach, $\sigma = 0.125$ μm/sec^2, would raise the error to 19.1 cm. If instead the actual gravity is a factor of 2.4 smaller (18 percent GEM10–GEML2), the weight favoring the non-dynamic approach would degrade the solution from the possible 6.2 cm to 9.0 cm. The nominal optimum weight of $\sigma = 0.5$ μm/sec^2 would yield 7.7 cm, which is only marginally better. Therefore, a biased weight favoring the non-dynamic approach (using a larger σ) is preferable when the level of dynamic error cannot be well determined.

B. A Gravity Adjustment Strategy

We now turn to a somewhat different approach in the form of a strategy specialized for a particular class of orbit and for strictly non-real-time application. The orbit must feature a regularly repeating ground track and must be at an altitude between roughly 600 and 3000 km, where gravity is the dominant dynamic error. Orbits for most earth observation satellites requiring high accuracy tracking, including Seasat, Topex, and ERS-1, fit these conditions. The technique features a novel gravity-adjustment strategy which exploits the special character of the orbit to achieve accuracy and efficiency.

Ordinarily the earth's gravity field is represented by a spherical harmonic expansion, and ordinarily several hundred coefficients are needed to support precise dynamic tracking of a low orbiter. Gravity "tuning," which is frequently carried

out to improve orbit accuracy, involves the adjustment of selected harmonic coefficients as part of the orbit determination process. Resonant components with large effects on a particular satellite orbit can thereby be improved, giving the desired orbit improvement.

Here we dispense with the harmonic representation and substitute a set of local parameters, or "bins," spaced evenly around each full ground track. For the fitting process, data from a large number of repeat ground tracks are collected in an ensemble. The user states at the beginning of each arc are estimated together with a single set of 3-D position corrections. These corrections correspond to orbit perturbations in each bin, common to all repeat arcs, that are due to gravity mismodeling, as illustrated in Fig. 14. Because the gravity perturbations felt by the user are the same for repeat ground tracks, collecting repeat orbits in an ensemble permits accurate recovery of local gravity effects by averaging random and other non-repeating errors. The number of parameters needed for the entire globe, and hence the effective gravity resolution, is roughly the same as with a harmonic expansion. With this approach, however, only the relatively few parameters pertaining to a particular ground track are dealt with at one time.

The mathematical details are given in [29] and [30]. Here we present a brief summary. Let $r(t)$ be the deviation of the orbiter position from a nominal trajectory and let t_j^i represent the jth time point of the ith trajectory in the ensemble, where $i = 1, 2, \ldots, N$ and $j = 1, 2, \ldots, M$. Then we can write the linearized expression

$$r(t_j^i) = \frac{\partial r}{\partial r_0} r_0^i + \frac{\partial r}{\partial v_0} v_0^i + \frac{\partial r}{\partial p^i} p^i + d_j \qquad (9)$$

where r_0 and v_0 are the deviations in epoch position and velocity, p^i represents the effects of all non-gravitational dynamic parameters, and d_j is the local parameter, common to all arcs, representing the position correction due to gravity mismodeling at that point. Solving for the d_j in the fitting process constitutes the gravity adjustment performed by this technique. We can write the above equation in matrix form as

$$R^i = (Vx_0)^i + d \qquad (10)$$

where R^i is the vector of position corrections for each time point in the ith arc, x_0 is the correction to the epoch state vector for the ith arc, V is the corresponding matrix of variational partials, d is the arc-independent vector of position corrections due to gravity mismodeling, and the non-gravitational terms p have been omitted. The a priori covariance of d can be derived from the gravity field used for the nominal trajectory

by means of a transformation matrix of variational partial derivatives, as described in [30]. Combining measurement data from the multiple data arcs, we can write the standard regression equation

$$z = Ax + n \qquad (11)$$

where z is the measurement vector, n is the data noise vector, x is the vector of parameters (including GPS states) to be estimated, and A is the matrix of measurement partials. Note that both A and x can be partitioned into arc-dependent and arc-independent parts. An efficient method of solving the partitioned regression equation by application of the Householder transformation is given in [29].

Although perhaps it isn't immediately evident, this is an extension of the non-dynamic strategy to repeating data arcs. As presented, the technique yields solutions for satellite epoch states in each arc plus arc-independent user position corrections in each gravity bin. In the degenerate case of a single data arc, however, the notion of arc-independent parameters collapses, and we can obtain a simple set of geometric position corrections—the $r(t_j)$ defined above. This, in essence, is the non-dynamic technique.

Results from a covariance analysis of this technique applied to the Topex example are presented in Figs. 15 and 16. The analysis examines ensembles of repeat tracks ranging in number from one to 100 and employs the same assumptions used in the analyses of Section 4, Subsection B. Figure 15 presents the total error from all sources, while Fig. 16 gives the error from data noise alone. As expected, the single-track case, represented by the top curve in each figure, gives the same result as the non-dynamic technique (not shown) for that arc, an average altitude error of about 8 cm. Performance improves rapidly with the first few additional arcs and then levels off at about 5 cm for a large number of arcs. The limiting error is the 5 cm error in each component assumed for the ground receivers, which contributes 4.9 cm of the total. Note in Fig. 16 that the data noise contribution continues to improve with added data, falling below 1 cm for 100 arcs. Current estimates for the error of our best known global reference points are in the range of 10 cm per component. Projections are that by the early to mid-1990s, many global points will be determined to 2 or 3 cm with improved VLBI and satellite laser ranging techniques. This would lead to a corresponding improvement in the performance shown in Fig. 15.

A further application of the repeat track concept lies in the improvement of gravity models. Finite time-differencing of the arc-independent position corrections yields local gravity

parameters. These can be collected from all ground tracks in the repeat sequence, and by application of suitable transformations, a conventional harmonic gravity model can be produced which is tailored for the particular orbit. Because data from the repeat ground tracks have been reduced to a small set of parameters, the final transformation to a global representation is computationally efficient. Resolution and accuracy will be essentially the same as with other techniques using the same set of data. Analysis for the Topex orbit indicates that with 100 repeat arcs for each ground track, a gravity field at Topex altitude can be recovered with an accuracy of 0.04 milligal and a resolution equivalent to a 12 X 12 spherical harmonic field. The accuracy will improve for lower values of degree and order and will fall off rapidly for higher values. For satellites at lower altitudes, much greater sensitivities can be achieved, particularly for terms of higher degree and order.

V. Summary and Conclusions

We have described five approaches to differential GPS tracking of low earth satellites. The purely geometric strategy is by far the most limited and is included here primarily for illustration and completeness. The general form, in which GPS orbits are adjusted, is capable in principle of near-decimeter performance but requires a prohibitive number of ground sites. The simple form, without GPS adjustment, is practical but limited to meter-level performance. Since it is operationally the simplest technique, geometric tracking may be the method of choice for missions requiring meter-level accuracy.

Fully dynamic tracking, whether with GPS or with another system, can offer decimeter accuracy only so long as dynamic modeling errors are adequately contained. For Topex, the dominant error is in the earth gravity model, and continued success in the current gravity improvement effort will be needed to reach a decimeter. For satellites at lower altitudes, such as NROSS, ERS-1, and EOS, decimeter gravity modeling will present a greater challenge; at the lowest altitudes, where

atmospheric drag is dominant, decimeter modeling is far out of reach.

The non-dynamic strategy, with its geometric user solution and dynamic GPS solution, is the first to offer practical subdecimeter accuracy at all altitudes and to dynamically active vehicles. Moreover, with no high-fidelity user models to compute, it is operationally simpler than a dynamic approach. It suffers, however, from a natural sensitivity to weak observing geometry, making it vulnerable to various forms of system degradation which can cause it to fail altogether.

Two rather different extensions of the non-dynamic strategy shore up this weakness by bringing more information to bear. The reduced-dynamic strategy is a sophisticated hybrid bringing together the dynamic and non-dynamic techniques in an optimal combination that can be continuously varied from fully dynamic to non-dynamic. Extensive analysis shows that this strategy must always be equal to or better than either technique separately and that it will enjoy its greatest success when dynamic performance and non-dynamic performance are comparable.

The gravity adjustment strategy is designed to exploit efficiently the information in an ensemble of repeat ground tracks. In general, each arc of the ensemble will reflect a different pattern of GPS satellite formations. The resulting set of position corrections, common to all arcs, will therefore be less sensitive to momentary weaknesses in GPS geometry. (Geographically correlated weaknesses due to ground site distribution will of course persist.) This is a specialized technique which may be of benefit to missions like Topex with a suitable orbit and a delayed processing schedule. For general applications, however, the optimized reduced dynamic strategy appears to be the strongest option. Though somewhat more complex operationally than classical dynamic orbit determination, it offers subdecimeter accuracy to all low orbiters, minimal sensitivity to dynamic and geometric weaknesses, and the versatility to adapt to changing conditions.

Acknowledgment

References

[1] G. H. Born, C. Wunch, and C. A. Yamarone, "TOPEX: Observing the Oceans from Space," *EOS Trans.*, vol. 65, pp. 433–437, July 10, 1984.

[2] G. H. Born, R. H. Stewart, and C. A. Yamarone, "TOPEX–A Spaceborne Ocean Observing System," in *Monitoring Earth's Ocean, Land, and Atmosphere from Space–Sensors, Systems, and Applications*, A. Schnapf, ed., New York: American Institute of Aeronautics and Astronautics, Inc., 1985.

[3] B. D. Tapley and J. C. Ries, "Orbit Determination Requirements for Topex," AAS Paper 87-429, presented at the AAS/AIAA Astrodynamics Specialist Conference, Kalispell, Montana, August 1987.

[4] M. H. Freilich, *The Science Opportunities using the NASA Scatterometer on NROSS*, JPL Publication 84-57, Jet Propulsion Laboratory, Pasadena, California, February 1, 1985.

[5] R. Holdaway, "Assessing Orbit Determination Requirements for ERS-1," AIAA Paper 86-0403, presented at the AIAA 24th Aerospace Sciences Meeting, Reno, Nevada, January 1986.

[6] K. F. Wakker, R. C. A. Zandbergen, and B. A. C. Ambrosius, "Seasat Orbiter Determination Experiments in Preparation for the ERS-1 Altimetry Mission," AAS Paper 87-426, presented at the AAS/AIAA Astrodynamics Specialist Conference, Kalispell, Montana, August 1987.

[7] R. Hartle and A. Tuyahov, "The Earth Observing System," AAS Paper 85-397, presented at the AAS/AIAA Astrodynamics Specialist Conference, Vail, Colorado, August 1985.

[8] B. G. Williams, "Precise Orbit Determination for NASA's Earth Observing System Using GPS," AAS Paper 87-409, presented at the AAS/AIAA Astrodynamics Specialist Conference, Kalispell, Montana, August 1987.

[9] R. J. Milliken and C. J. Zoller, "Principles of Operation of NAVSTAR and System Characteristics," *Navigation*, vol. 25, pp. 95–106, summer 1978.

[10] J. J. Spilker, "GPS Signal Structure and Performance Characteristics," *Navigation*, vol. 25, pp. 121–146, summer 1978.

[11] M. P. Ananda and M. R. Chernick, "High Accuracy Orbit Determination of Near-Earth Satellites using Global Positioning System (GPS)," in *Proceedings, IEEE PLANS '82*, pp. 92–98, 1982.

[12] S. C. Wu and V. J. Ondrasik, "Orbit Determination of Low-Altitude Earth Satellites using GPS RF Doppler," in *Proceedings, IEEE PLANS '82*, pp. 82–91, 1982.

[13] T. P. Yunck, W. G. Melbourne, and C. L. Thornton, "GPS-Based Satellite Tracking System for Precise Positioning," *IEEE Trans. Geosci. and Remote Sensing*, vol. GE-23, no. 4, pp. 450–457, July 1985.

[14] S. M. Lichten, S. C. Wu, J. T. Wu, and T. P. Yunck, "Precise Positioning Capabilities for TOPEX using Differential GPS," AAS Paper 85-401, presented at the AAS/AIAA Astrodynamics Specialist Conference, Vail, Colorado, August 1985.

[15] T. P. Yunck, S. C. Wu, and S. M. Lichten, "A GPS Measurement System for Precise Satellite Tracking and Geodesy," *J. Astronautical Sci.*, vol. 33, no. 4, pp. 367–380, October–December 1985.

[16] W. G. Melbourne and E. S. Davis, "GPS-Based Precision Orbit Determination: A Topex Flight Experiment," AAS Paper 87-430, presented at the AAS/AIAA Astrodynamics Specialist Conference, Kalispell, Montana, August 1987.

[17] T. P. Yunck and S. C. Wu, "Non-Dynamic Decimeter Tracking of Earth Satellites using the Global Positioning System," AIAA Paper 86-0404, presented at the AIAA 24th Aerospace Sciences Meeting, Reno, Nevada, January 1986.

[18] S. C. Wu, S. M. Lichten, and T. P. Yunck, "Gravity Mismodelling on Topex Orbit Determination," AAS Paper 86-2056-CP, presented at the AIAA/AAS Astrodynamics Specialist Conference, Williamsburg, Virginia, August 1986.

[19] S. C. Wu, T. P. Yunck, and C. L. Thornton, "Reduced-Dynamic Technique for Precise Orbit Determination of Low Earth Satellites," AAS Paper 87-410, presented at the AAS/AIAA Astrodynamics Specialist Conference, Kalispell, Montana, August 1987.

[20] F. J. Lerch, S. M. Klosko, R. E. Laubscher, and C. A. Wagner, "Gravity Model Improvement using GEOS 3 (GEM 9 and 10)," *J. Geophys. Res.*, vol. 48, no. B8, pp. 3897–3916, July 1979.

[21] F. J. Lerch, B. H. Putney, C. A. Wagner, and S. M. Klosko, "Goddard Earth Models for Oceanographic Applications (GEM 10B and 10C)," *Marine Geodesy*, vol. 5, no. 2, pp. 145–187, 1981.

[22] F. J. Lerch, S. M. Klosko, G. B. Patel, and C. A. Wagner, "A Gravity Model for Crustal Dynamics (GEM-L2)," *J. Geophys. Res.*, vol. 90, no. B11, pp. 9301–9311, September 1985.

[23] G. Rosborough, "Orbit Error Due to Gravity Model Error," AAS Paper 87-534, presented at the AAS/AIAA Astrodynamics Specialist Conference, Kalispell, Montana, August 1987.

[24] T. Meehan *et al.*, "Rogue: A New High Accuracy Digital GPS Receiver," presented at the International Union of Geodesy and Geophysics Nineteenth General Assembly, Vancouver, Canada, August 1987.

[25] Y. Bock, S. A. Gourevitch, C. C. Counselman III, R. W. King, and R. I. Abbot, "Interferometric Analysis of GPS Phase Observations," in *Proc. Fourth Int. Geodetic Symp. on Satellite Positioning*, Austin, Texas, April 1986.

[26] G. Blewitt, "New Approaches to Carrier Phase Ambiguity Resolution and the Benefits of Simultaneous Fits to Phase and Group Delay Observables," presented at the International Union of Geodesy and Geophysics Nineteenth General Assembly, Vancouver, Canada, August 1987.

[27] G. J. Bierman, *Factorization Methods for Discrete Sequential Estimation*, New York: Academic Press, 1977.

[28] S. C. Wu and C. L. Thornton, "OASIS—A New GPS Covariance and Simulation Analysis Software System," in *Proc. First Int. Symp. on Precise Positioning with GPS*, pp. 337–346, May 1985.

[29] J. T. Wu, "TOPEX Orbit Determination by Solving Gravity Parameters with Multiple Arcs," AAS Paper 85-411, presented at the AAS/AIAA Astrodynamics Specialist Conference, Vail, Colorado, August 1985.

[30] J. T. Wu and S. C. Wu, "TOPEX Orbit Determination by Combining GPS Data from Repeat Orbits," AIAA Paper 86-2216-CP, presented at the AIAA/AAS Astrodynamics Specialist Conference, Williamsburg, Virginia, August 1986.

Table 1. Error model and other assumptions used in covariance analysis

User satellite	Topex (1334 km in altitude)
Number of stations	6 (cf. Fig. 2)
Number of GPS satellites	18
Cutoff elevation	10 degrees at stations 0 degrees at Topex
Data type	P-code pseudorange carrier phase
Data span	2 hours
Data interval	5 minutes
Data noise	5 cm (pseudorange) 0.5 cm (carrier phase)
Carrier phase bias	10 km (adjusted)
Clock bias	3 μsec (adjusted as white process noise)
Topex epoch state	2 km; 2 m/sec (adjusted)
GPS epoch states	2 m; 0.2 mm/sec (adjusted)
Station location	5 cm each component
Zenith troposphere	1 cm
Earth's GM	1 part in 10^8
Gravity	Scaled GEM10–GEML2 (20 × 20 lumped)
Solar pressure	10 percent
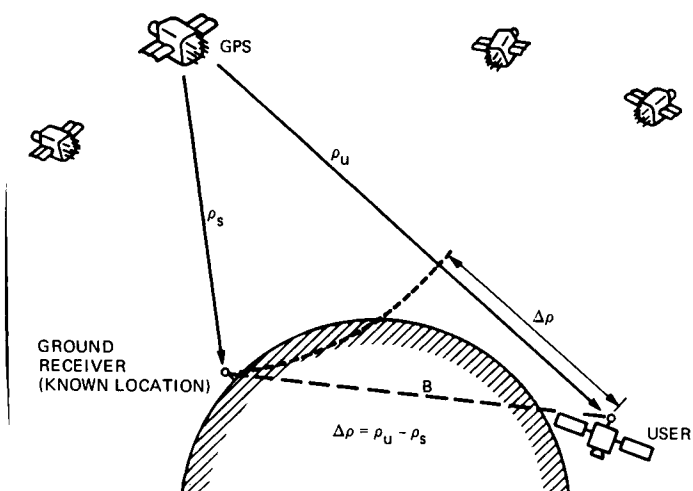
Fig. 1. Differential pseudorange observations to four GPS satellites provide position and time offset with respect to the ground reference point, resulting in substantial cancellation of GPS errors
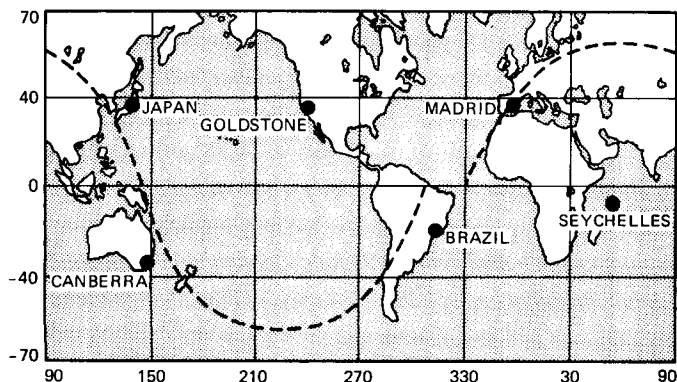
Fig. 2. GPS ground receiver sites used in error studies and one-orbit Topex ground track
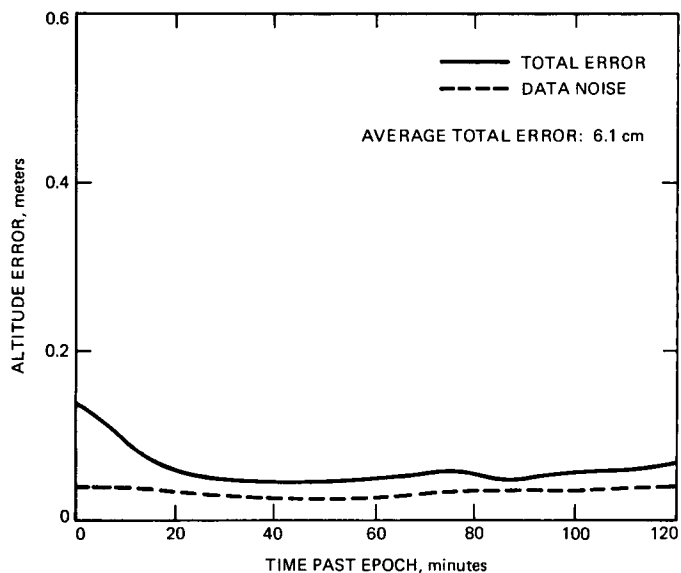
Fig. 3. Predicted Topex altitude error with dynamic differential GPS tracking using an optimistic gravity error model
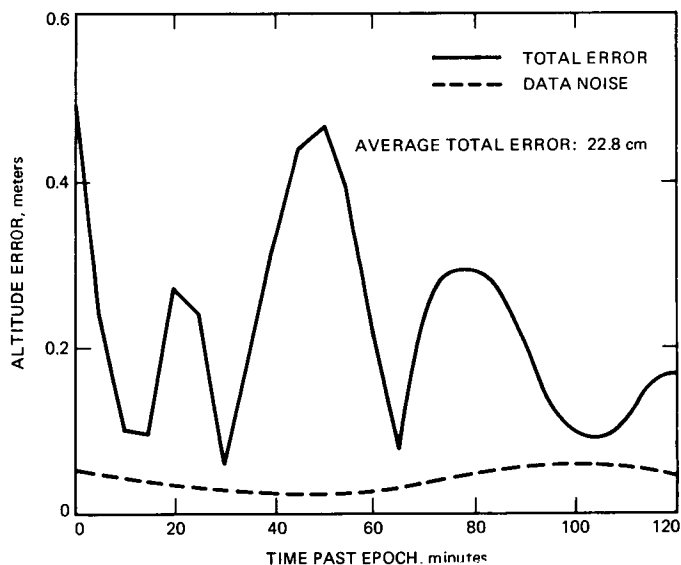
Fig. 4. Predicted Topex altitude error with dynamic differential GPS tracking using a pessimistic gravity error model (c. 1983)
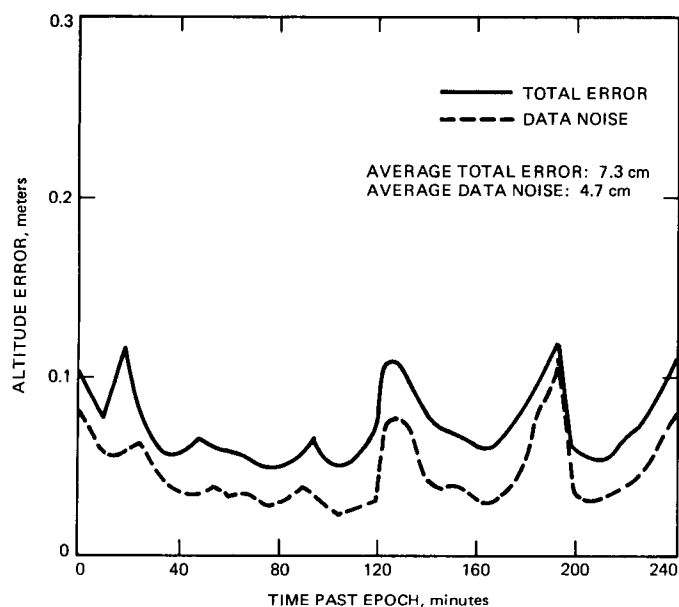
Fig. 5. Predicted Topex altitude error with the non-dynamic
strategy using the mixed data type
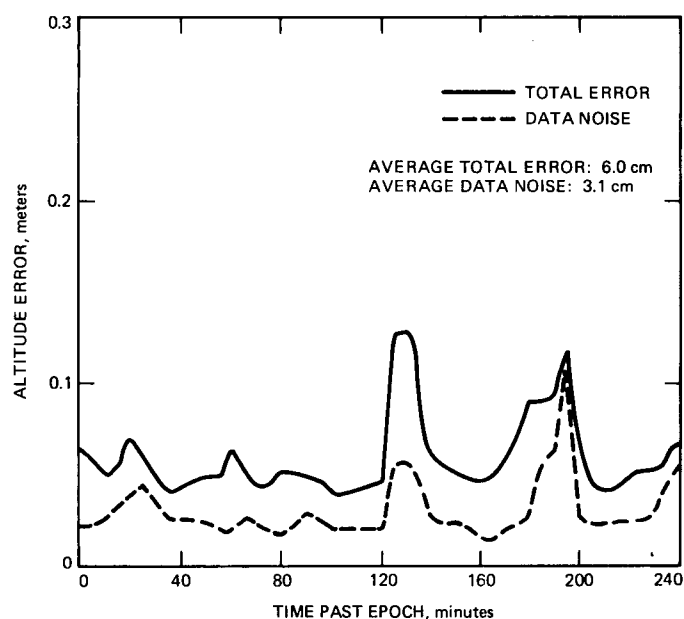
Fig. 6. Predicted Topex altitude error with the non-dynamic
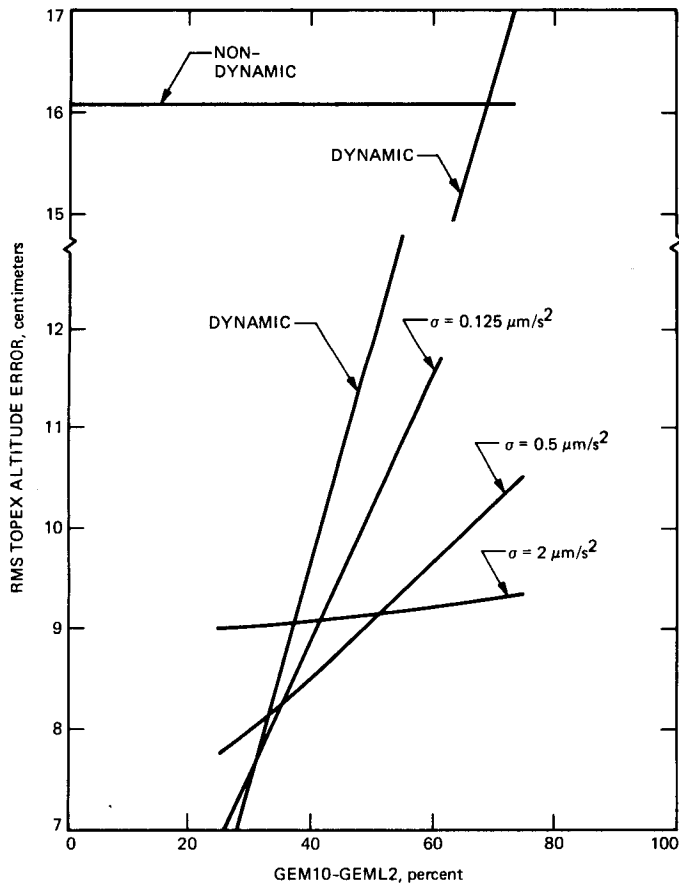strategy using differenced carrier range (τ = 15 minutes)
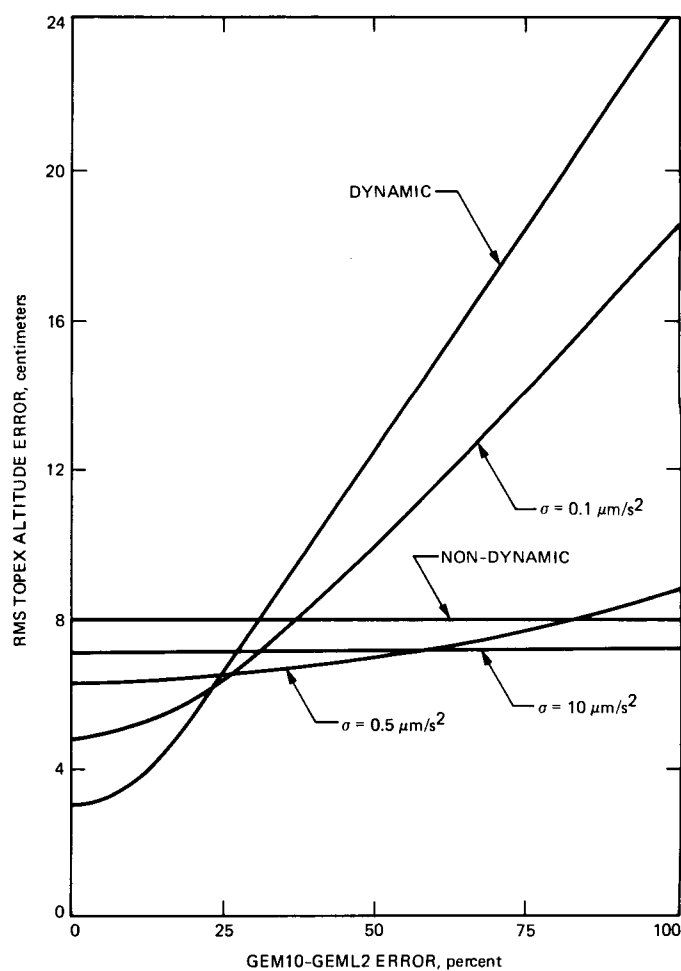
Fig. 7. Predicted Topex altitude error, assuming 6-satellite
viewing capacity, using dynamic, non-dynamic, and
reduced-dynamic strategies, shown as a function of gravity
model quality
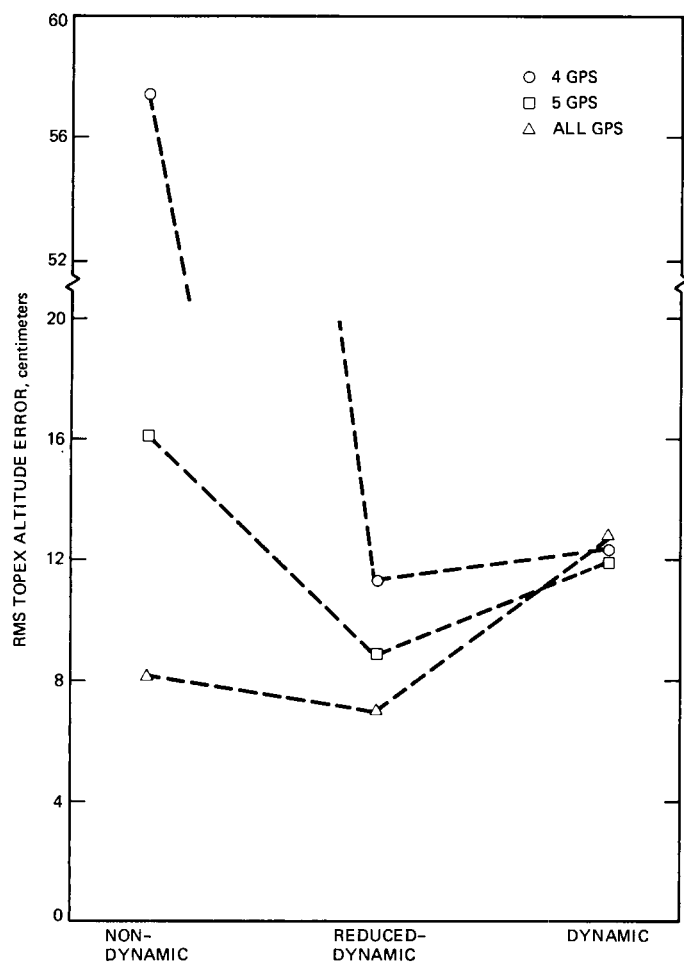
Fig. 8. Predicted Topex altitude error using dynamic, non-dynamic, and reduced-dynamic strategies, shown for three different flight receiver viewing capacities
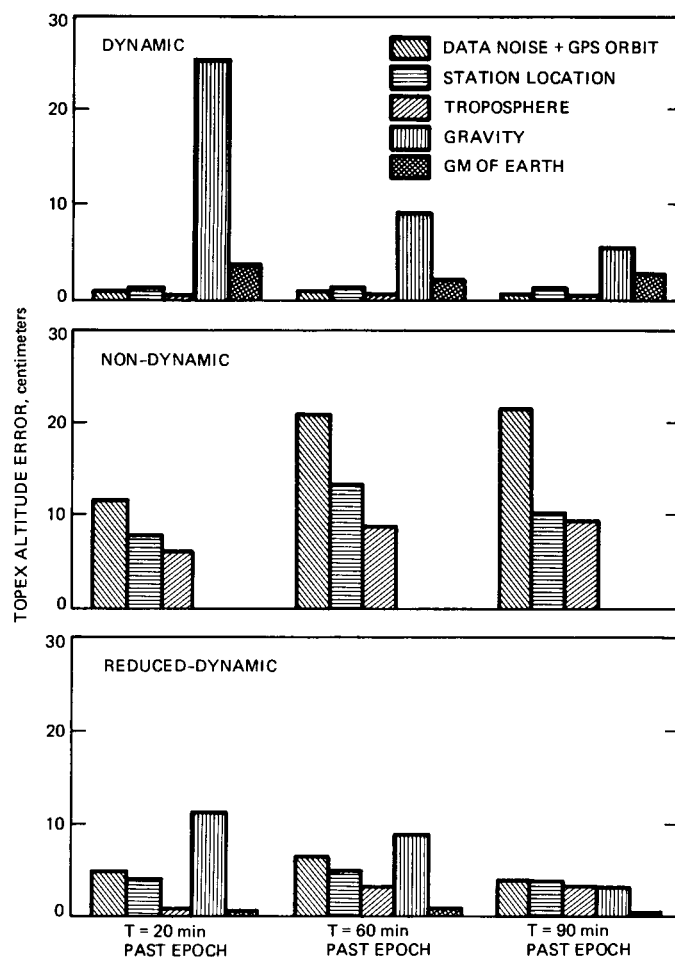
Fig. 10. Breakdown of predicted Topex altitude error at three peak points
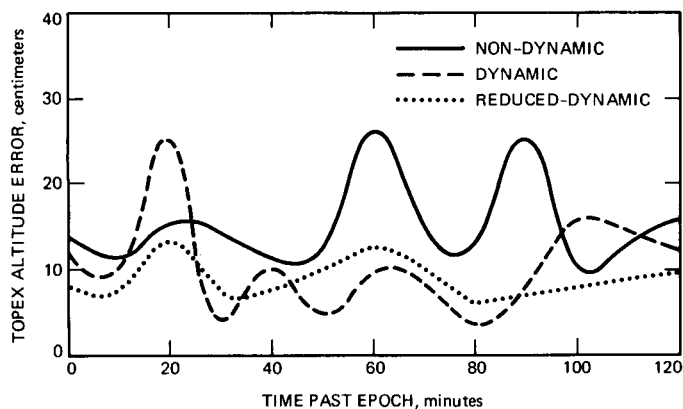
Fig. 9. Detail of predicted Topex altitude error over a full 2-hour data arc for dynamic, non-dynamic, and reduced-dynamic strategies
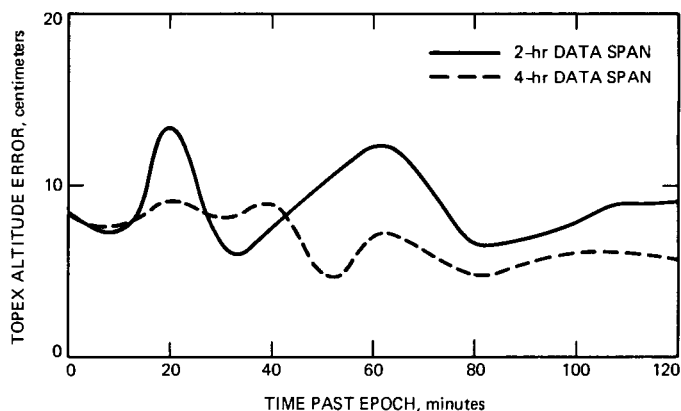
Fig. 11. Detail of predicted Topex altitude error with reduced-dynamic technique for 2-hour and 4-hour data spans

43

Fig. 12. Predicted Topex altitude error, assuming 5-satellite viewing capacity, using dynamic, non-dynamic, and reduced-dynamic strategies, shown as a function of gravity model quality
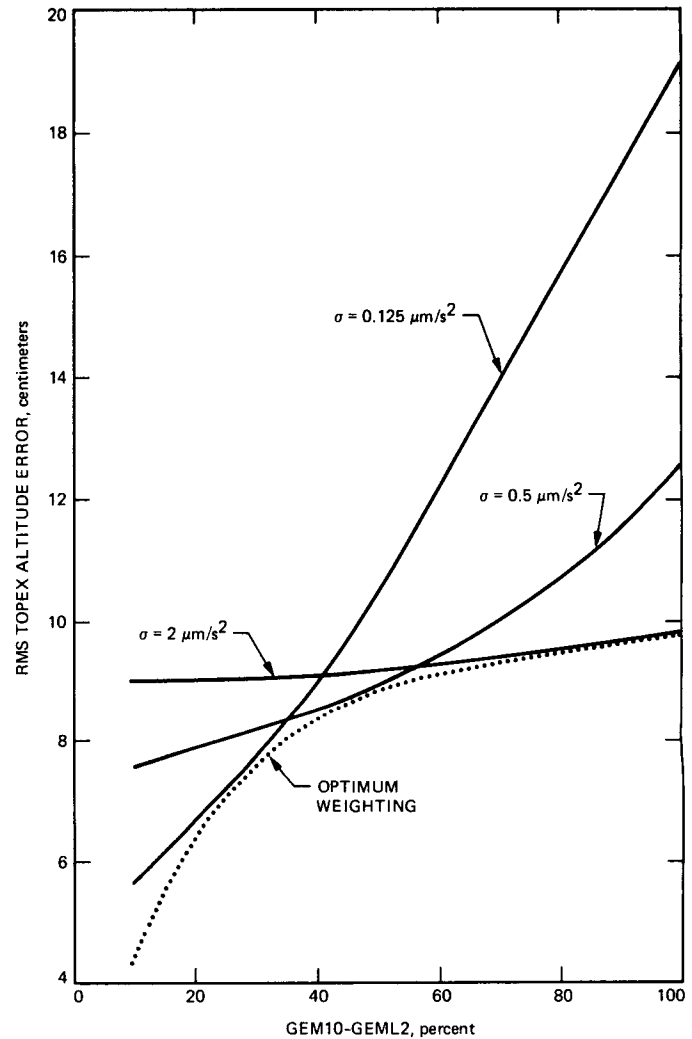

Fig. 13. Predicted Topex altitude error, assuming 5-satellite viewing capacity, with optimal reduced-dynamic weighting (dotted line), shown as a function of gravity model quality
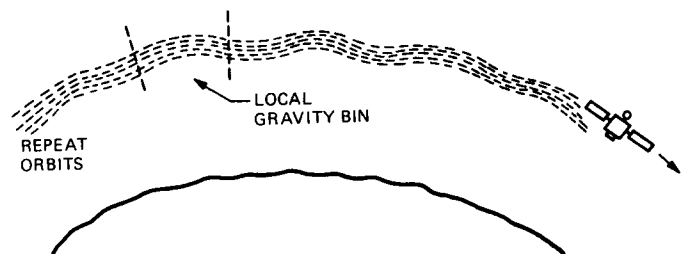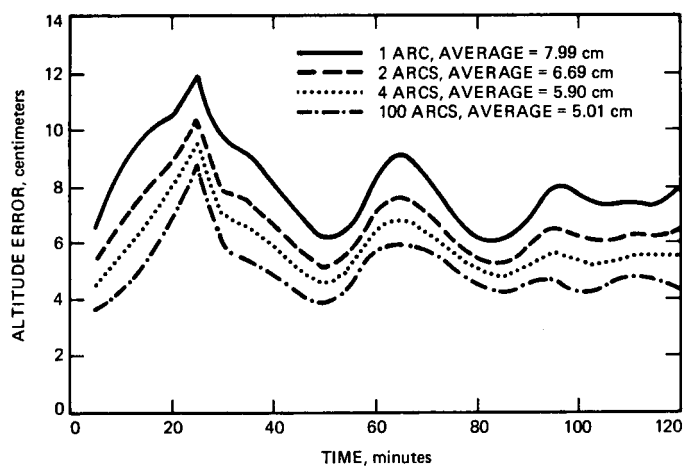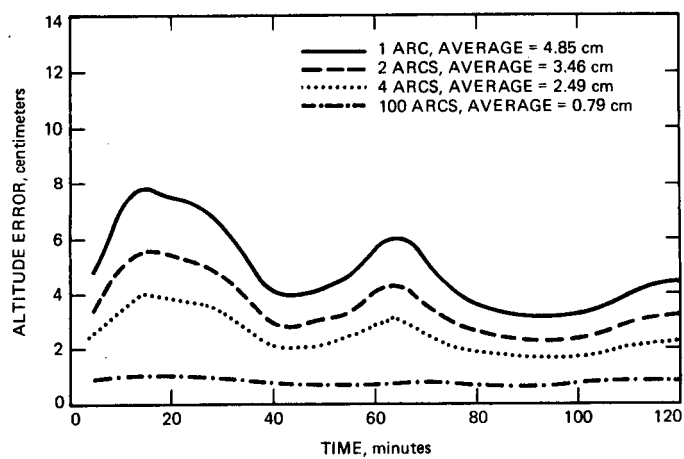

Fig. 14. The gravity adjustment strategy estimates local gravity parameters using data from repeat ground tracks

Fig. 15. Predicted Topex altitude error using gravity adjustment strategy, shown for ensembles of repeat arcs numbering from 1 to 100

Fig. 16. Data noise contribution to predicted Topex altitude error using the gravity adjustment technique